

How electron delocalization influences the electron-withdrawing properties of isomeric benzobischalcogenadiazoles

Elena O. Levina,^{*a,b} Ekaterina V. Bartashevich,^a Alexey E. Batalov,^a
Oleg A. Rakitin^{a,c} and Vladimir G. Tsirelson^{a,d}

^a South Ural State University, 454080 Chelyabinsk, Russian Federation.
E-mail: levina.eo@phystech.edu

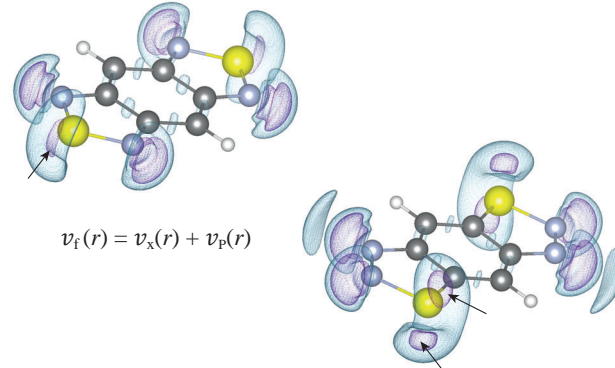
^b N. S. Kurnakov Institute of General and Inorganic Chemistry, Russian Academy of Sciences,
119991 Moscow, Russian Federation

^c N. D. Zelinsky Institute of Organic Chemistry, Russian Academy of Sciences, 119991 Moscow,
Russian Federation

^d D. I. Mendeleev University of Chemical Technology of Russia, 125047 Moscow, Russian Federation

DOI: 10.1016/j.mencom.2023.04.024

The fermionic potential and delocalization indices for benzobis-1,2,5-chalcogenadiazoles reveal inhomogeneous electron delocalization in their benzene ring, which results in compactly localized lone electron pairs on the chalcogen atoms. These features of (de)localization are rooted in a local increase in the kinetic component of the electron correlation, which expresses the Fermi hole variability and the kinetic potential response to electron density variations in the benzene ring of benzobis-1,2,5-chalcogenadiazoles. This explains their better electron-withdrawing properties compared to benzobis-1,2,3-chalcogenadiazoles.



Keywords: benzobischalcogenadiazoles, orbital-free DFT, electron delocalization indices, Fermi hole, electron acceptors.

Benzo-fused 1,2,3-chalcogenadiazoles (123CDs) and 1,2,5-chalcogenadiazoles (125CDs) belong to the class of practically important chalcogen–nitrogen heterocycles¹ and serve as moderately electron-deficient building blocks. Benzo[c][1,2,5]thiadiazole (BTD) occupies an exceptional place among them, as it has medical applications and, due to its electrical conductivity, can be used as a material for photovoltaic devices.² Benzo[d][1,2,3]thiadiazole (isoBTD) resembles BTD in both properties and structure, although much less studied.³ However, there is still a need for photovoltaic materials with better specific characteristics (*e.g.*, narrower bandgap). To achieve this, it is necessary to design ultra electron-withdrawing building blocks for them, such as heteroannulated benzochalcogenadiazoles fused with other electron acceptors. Recent reviews have noted progress in the synthesis and applications of such tricyclic benzobischalcogenadiazoles (BBCDs).^{4–6}

In this work, we examined the features of the electronic structure of tricyclic BBCDs using novel chemical bonding descriptors and gave their physical and chemical interpretation. Our aim was to track the influence of electronic effects on their electron-withdrawing properties. Similar approaches have worked well for establishing the relationship between the electronic properties of five-membered N,S(Se)-heterocycles, such as thiazoles, thia-(selena)diazoles, dithiazoles and dithiadiazoles, and their reactivity.^{5,6} Features of electron delocalization and the corresponding bond orders in N,S-heterocyclic compounds were examined using electron delocalization indices.⁵ To study the electronic properties in Appel's salt crystal, one-electron orbital-free DFT potentials

were used.⁷ Here, we focused on studying the features of the electronic structure of tricyclic BBCDs using chemical bonding descriptors.

In quantum chemistry, electron delocalization descriptors such as delocalization indices (DIs) and the electron localization function, among others,^{8–13} are often determined *via* the Fermi hole, $h_x(r, r')$. It estimates the decrease in the probability of finding an electron with a given spin at point r' while a reference electron with the same spin is in position r . This function is a direct measure of the electron exchange correlation, which is responsible for the (de)localization of electrons in atomic-molecular systems.^{12,14–16} If $h_x(r, r')$ has a compact distribution somewhere and greatly changes its shape near this area, we treat that as the localization of an electron pair in this region of space. In contrast, if the Fermi hole is smeared and changes little with changing r in an extended region of space, then one can speak of a pronounced delocalization of the electron. Unfortunately, a direct analysis of the Fermi hole distribution in molecules is complicated by the dependence of $h_x(r, r')$ on two variables.

With the help of one-electron potentials, one can estimate two main characteristics of a Fermi hole, its depth and its tendency to change.¹⁷ The fermionic potential v_f , consisting of the exchange potential $v_x(r)$ and the Pauli potential $v_p(r)$:

$$v_f(r) = v_x(r) + v_p(r), \quad (1)$$

simultaneously reveals the manifestation of the Pauli exclusion principle both in the potential and in the kinetic electron energy density of the system, *i.e.*, in the static and kinetic contributions

to the electron correlation, respectively.^{17,18} The first v_f component, $v_x(r) < 0$, mainly depends on the average depth of the Fermi hole $h_x(r, r')$, weighted by the distance between points r and r' , and is negative throughout the space.^{18–20} The second component, $v_p(r) > 0$, characterizes the variability of the Fermi hole in the proximity of point r and the response of the kinetic potential to the electron density variation.²⁰ Regions with high values of v_p (and $v_f > 0$) indicate a fast change in the shape of the Fermi hole in their vicinity and a large response of the kinetic potential to density variations (the kinetic contribution to the electron correlation prevails over the static one). That is, regions with $v_f > 0$ indicate the proximity of areas where the electron localization changes rapidly.¹⁸ On the contrary, regions with $v_f < 0$ signal a high localization of electrons in these areas.¹⁸

The energy of the lowest unoccupied molecular orbital (ϵ_{LUMO}) in benzobis-1,2,5-chalcogenadiazoles (BB125CDs) was found to be ~ 0.8 eV lower than that in their analogs with 123CD rings (Table S1[†]). The difference in ϵ_{LUMO} between thia- and selenadiazoles is ~ 0.2 and 0.02 eV for BB125CDs and benzobis-1,2,3-chalcogenadiazoles (BB123CDs), respectively. These values agree well with the changes in the electron affinity of the considered compounds (see Table S1). In BB125CDs, the electron affinity is ~ 0.7 eV higher than in BB123CDs, and the substitution of S atoms for Se atoms leads to a change in electron affinity by 0.2 and 0.06 eV depending on whether BB125CD or BB123CD is being considered. This indicates that the position of the chalcogen (Ch) in the heterocyclic ring affects the electron-withdrawing properties of the considered compounds more than the nature of the Ch itself. In other words, BB125CDs are able to accept an electron more easily than BB123CDs. Bromo-substituted compounds demonstrate both an increase in electron affinity and a decrease in ϵ_{LUMO} by ~ 0.3 eV compared to unsubstituted BBCDs (see Table S1). This suggests that the substitution of hydrogen for halogen in both BB123CDs and BB125CDs enhances their electron-withdrawing properties.

To study how the features of electron delocalization influence the electron-withdrawing properties of the studied compounds, we analyzed the relationship between the sums of the DIs⁸ (ΣDI) over five- and six-membered rings in these molecules and the LUMO energy. The value of ϵ_{LUMO} serves as a simple indicator of electron-withdrawing properties, since it correlates well with electron affinity and reflects all tendencies of its changes for the considered

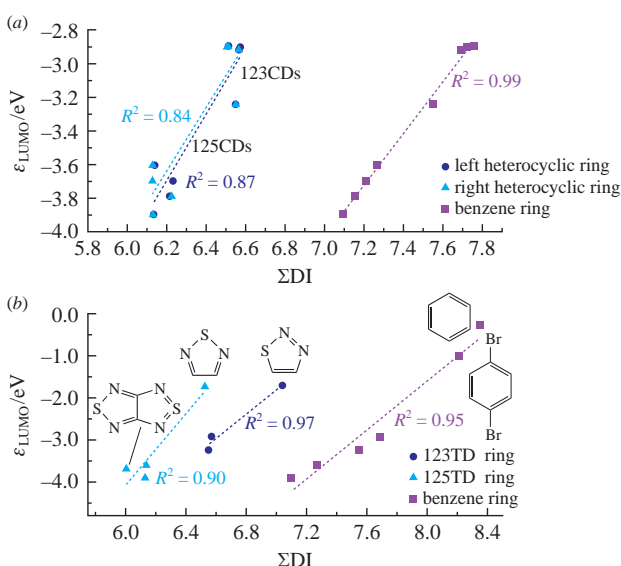


Figure 1 Relationships between the DIs (ΣDI) summed over the rings of the considered molecules and their LUMO energy.

[†] For details, see Online Supplementary Materials.

compounds (see Table S1). Particularly good correlations were obtained for the ΣDI calculated for the benzene ring, as well as for heterocyclic moieties [Figure 1(a)]. They clearly indicate a tendency for the LUMO energy to decrease with decreasing electron delocalization in the benzene and heterocyclic moieties. Calculations performed with benzobisthiadiazoles, benzene itself, 1,4-dibromobenzene, 1,2,3-thiadiazole (123TD), 1,2,5-thiadiazole (125TD) and bis(1,2,5-thiadiazole) confirm that this behavior seems to be common not only for BBCDs, but also for other aromatic molecules structurally similar to BCDA fragments [Figure 1(b)]. It is important to note that the dots on the dependences of ϵ_{LUMO} on ΣDI of BBCDs [see Figure 1(a)] are grouped into two clusters. 125CDs with lower LUMO levels demonstrate poorer electron delocalization for both heterocyclic and benzene moieties compared to 123CDs. It emerged that this is mostly due to changes in the number of shared electrons for several specific fragments in BBCDs (Figure 2).

The relatively large DI values for the N–S bonds in the 125CD fragments do not compensate for the high DI values of the formally double N–N bond in the BB123CD rings. For the C–C bond, which belongs to both carbo- and hetero-cycles, the DI values are systematically lower in BB125CDs. This bond also contributes to an increase in the magnitude of electron delocalization in both five- and six-membered rings of BB123CDs.

To study the physical nature of the effects leading to greater or lesser delocalization of electrons in BB123CDs and BB125CDs, we applied the analysis of one-electron potentials. We started by studying the fermionic potential v_f , which measures the influence of both the static and kinetic components of the electron correlation (effects contributing to the potential and kinetic energy densities) on the (de)localization of electron pairs in the system [equation (S1)[†]]. Its distribution in the π -plane of the C–C bond fusing the benzene and heterocyclic moieties [Figure 3(a)][†] confirms the poorer electron delocalization in this area for BB125CDs. The electrons tend to localize on the C–C bond, which manifests itself in more pronounced negative values of v_f there (deeper Fermi hole). The higher v_f barrier (more positive v_f values) above and below the C–C bond reflects the higher variability of Fermi holes near this region and the higher response of the kinetic potential to small variations in electron density. This makes the electron delocalization in the benzene ring of BB125CDs more inhomogeneous. The Fermi-hole dependent part,

$$v_f^{\text{hole}}(r) = \int [h_x(r, r')/|r-r'|] dr' + (1/2) \int |\nabla_r f(r, r')|^2 dr', \quad (2)$$

demonstrates that both of the mentioned effects influence the v_f barrier [Figure 3(b)].[†] Its negative values above and below the C–C bond in 123CDs are more broadly and homogeneously

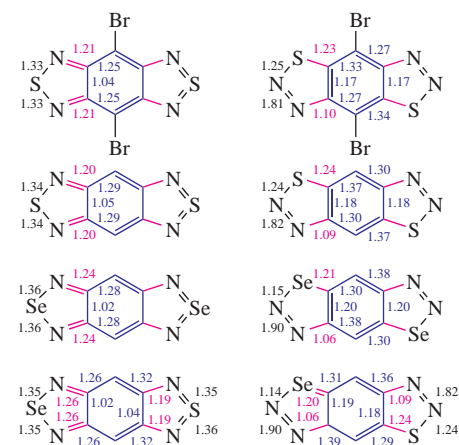


Figure 2 DI values for bonds in BB125CDs and BB123CDs. Identical DI values for symmetrical parts of the molecules are omitted.

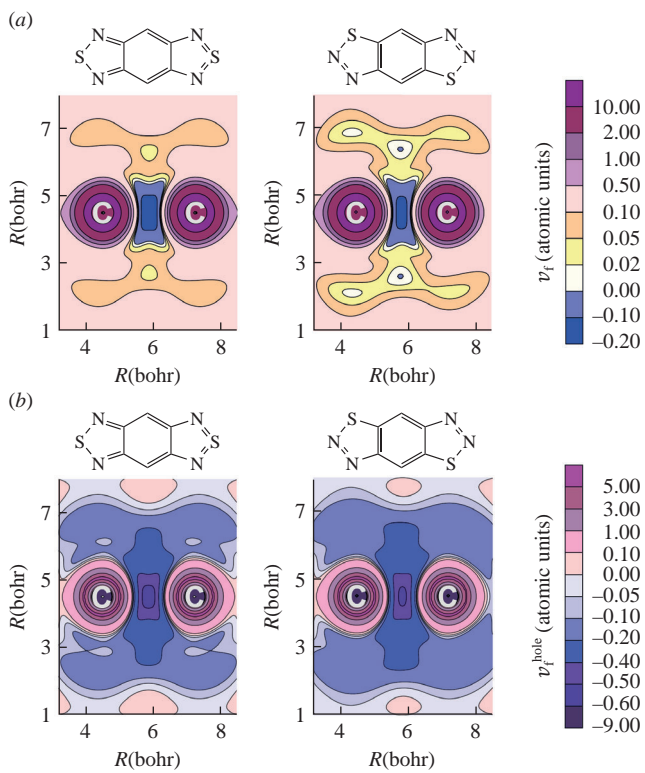


Figure 3 Distributions of (a) the fermionic potential $v_f(r)$ and (b) its Fermi-hole dependent part $v_f^{\text{hole}}(r)$ [equation (2)] in the plane orthogonal to the molecular plane and passing through the C–C bond that fuses the benzene and heterocyclic rings in benzobisthiadiazoles.

distributed, which indicates a lower Fermi hole variability there and stipulates electron delocalization in the π -plane of the benzene ring.

The inhomogeneous delocalization of electrons in the benzene ring of BB125CDs (see Figures 2 and 3) also affects other electron-rich regions of the molecules. One can see that the value of v_f in the plane of the five-membered ring becomes less negative for N lone pairs compared to isolated heterocycles (Figure 4). On the contrary, BB123CDs retain the intensity of N lone pairs' localization characteristic of their non-fused analogs. In BB125CDs, the localization of Ch lone pairs also becomes atypical. They form a single domain behind the S atom in the heterocyclic plane, while S lone pairs are normally localized as two separate domains above and below the plane of the heterocyclic molecule (Figure 5). In benzobis-1,2,5-selenadiazoles, the domains corresponding to the Se lone pairs are less negative and less bulky than in benzobis-1,2,3-selenadiazoles (Figure S3[†]). Importantly, these effects cannot be attributed to the Ch atom position in the heterocyclic fragment alone, since non-fused 125CDs retain the usual localization of Ch lone pairs.

To answer the question whether these features are caused only by the intensity of electron delocalization in benzene or also by the heterocyclic moieties, we consider the distributions of one-electron potentials in the heterocyclic fragments (Figures 4, S2 and S4). Positive values of v_f on the S–N (Se–N) and N–N bonds indicate that the kinetic response part of v_f [equations (S2) and (S4)] dominates the Fermi-hole dependent part of v_f (Figure S2). As a result, it completely surpasses v_x , which reflects the depth of the Fermi holes on these bonds [equation (S3)]. However, to analyze the contribution of electron pair localization to the covalent bond component (Fermi hole depth) in the heterocyclic moieties, it suffices to consider only the v_x distribution²¹ (see Figure S4). It confirms the increase in the localization of electron pairs on the N–N bond of benzobis-1,2,3-thiadiazoles compared to the two S–N bonds of their analogs with the 125TD rings, suggested by DIs. This feature is a direct consequence of the heterocyclic

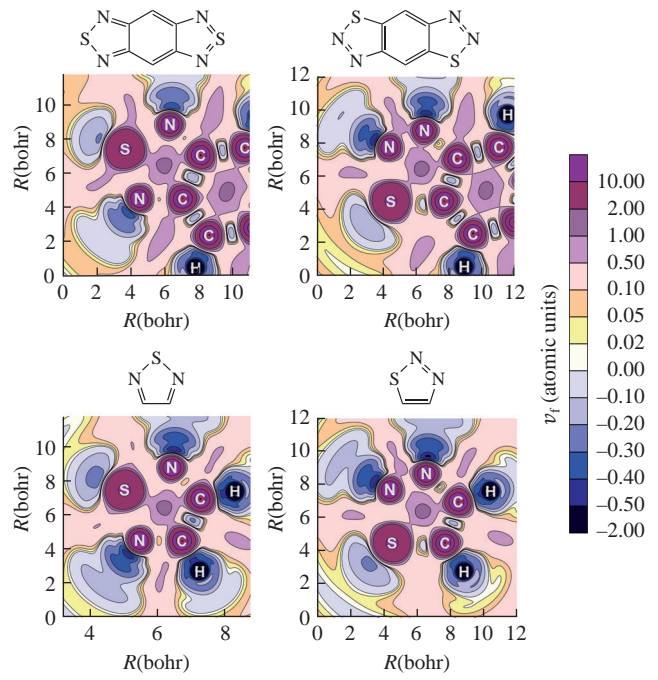


Figure 4 Distribution of the fermionic potential v_f in the plane of the heterocyclic moieties for non-fused 123TDs and 125TDs and their benzobisthiadiazole analogs.

structure, which can be easily demonstrated by comparing the v_x maps plotted for fused and non-fused chalcogenadiazoles (see Figure S4). In both cases, the localization of electron pairs, due to the static component of the electron correlation, has similar features and magnitude. Since the localization of the S(Se) and N lone pairs is different in BB125CDs and their non-fused analogs, these changes cannot be influenced by the static contribution to the electron correlation in the heterocyclic moieties. That is, an increase in the kinetic contribution to the electron correlation leads to an increased barrier of the v_f potential at the C–C bond fusing the heterocyclic and benzene moieties and affects the (de)localization of electrons there. It causes the S(Se) lone pairs to localize as more compact domains in BB125CDs. For thiadiazoles, it even makes the electron distribution around the S atom more peculiar than the typical picture for sp^3 and sp^2 hybridization of chalcogens. The S–N bonds in benzobis-1,2,5-thiadiazoles can be considered as a hybrid of single and double bonds, which perfectly agrees with previous findings.²² The DIs, proportional to bond orders^{5,23} confirm this interpretation (see Figure 2).

Taking into account all the described features of the electron distribution in different chalcogenadiazoles, it should be recalled that non-fused 123TDs and 125TDs have almost no difference in their LUMO energy (see Figure 1). This suggests an interdependence between the $\varepsilon_{\text{LUMO}}$ lowering in 1,2,5-benzothiadiazoles and abrupt changes in electron delocalization in the benzene ring of these molecules. Also, this is expressed numerically in the perfect correlations of $\varepsilon_{\text{LUMO}}$ with DIs summed over the benzene ring (see Figure 1). Analysis of the one-electron potentials showed that these changes are governed by the kinetic contribution to the electron correlation in the π -plane of the benzene ring. This effect also leads to the depletion of electron localization in other electron-rich areas of BB125CDs. In other words, the increasing kinetic contribution to the electron correlation in the π -plane near the bond fusing the benzene and heterocyclic moieties of BB125CDs enhances the electron-withdrawing properties of these molecules.

The electron-withdrawing sites of BBCDs can be explicitly visualized (Figure 6) through the distribution of the Fukui function $f^+(r)$.²⁴ It was found that, regardless of the position of the Ch in the heterocyclic moieties, the two benzene carbons in positions 4 and 8

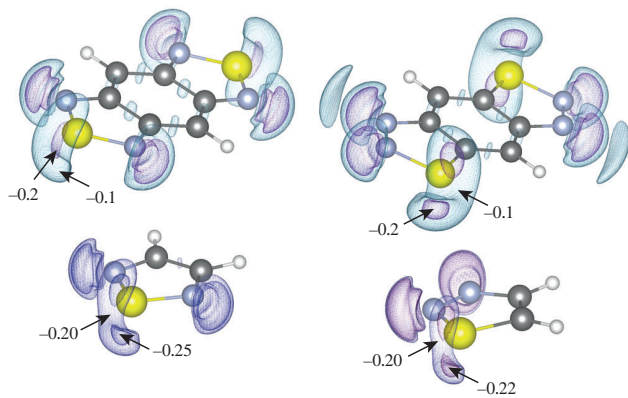


Figure 5 3D surfaces and explicit values (atomic units) of the fermionic potential v_f for 123TDs and 125TDs and their benzobisthiadiazole analogs. Negative artifacts near H nuclei are not shown. Atoms C, N, S and H are shown in gray, blue, yellow and white, respectively.

are favorable for nucleophilic attack, as evidenced by the positive parts of the Fukui function f^+ . However, the distribution of f^+ in heterocyclic moieties differs greatly for the five-membered rings of 123CDs and 125CDs. In BB123CDs, the Ch atom loses its electron-withdrawing properties, while in BB125CDs it serves as a possible site of nucleophilic attack. The non-fused chalcogenadiazoles retain electron-withdrawing areas on the S(Se) and N atoms, regardless of the position of the Ch in the heterocycle. This peculiarity of BB123CDs can be explained by the spatial localization of the electron pairs of their Ch. Although both non-fused chalcogenadiazoles and BB123CDs have two domains in which electron pairs are localized, in the latter these domains are further apart, resulting in bulky lone pairs (see Figures 5 and S3). They propagate above and below the heterocyclic plane, shielding the Ch atom from nucleophilic attack. This explains the deterioration of the electron-withdrawing properties of BB123CDs compared to their 125CD analogs. The bridged-type f^+ -positive areas above and below the C–N bond in BB123CDs also indicate the tendency of these compounds to cycloaddition reactions. Although this cannot be attributed to the influence of the benzene ring, since such a distribution of f^+ is also characteristic of non-fused 123CDs.

In conclusion, it should be emphasized that the proposed methodology showed how electron delocalization throughout the molecule controls the electron-withdrawing properties of isomeric benzobischalcogenadiazoles. It demonstrates the possibility of enhancing the electron-withdrawing properties of polycyclic compounds not only due to the spatial enlargement of the conjugated molecular core,²⁵ but also due to the isomerization of heterocyclic moieties that are part of the conjugated system. The combined

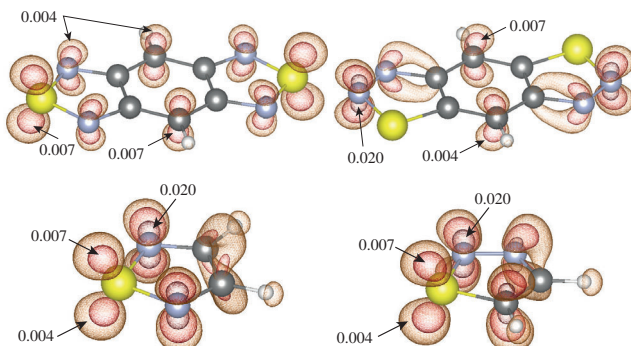


Figure 6 3D surfaces of the Fukui function $f^+(r)$ for values of 0.004, 0.007 and 0.020 atomic units in fused and non-fused 123TDs and 125TDs. The values of f^+ are explicitly indicated in the figure.

use of new tools for studying electron (de)localization, namely, one-electron potentials containing information on exchange correlation, with widely applied chemical bonding descriptors, such as delocalization indices and the Fukui function, can be fruitful for examining the features of delocalization in other promising Ch,N-heterocycles. One-electron potentials also help deepen understanding of electron (de)localization by directly measuring and comparing the physical effects that cause this phenomenon.

This research was supported by the Ministry of Science and Higher Education of the Russian Federation (project no. FENU-2020-0019).

Online Supplementary Materials

Supplementary data associated with this article can be found in the online version at doi: 10.1016/j.mencom.2023.04.024.

References

1. T. Chivers and R. S. Laitinen, *Chalcogen–Nitrogen Chemistry: From Fundamentals to Applications in Biological, Physical and Materials Sciences*, World Scientific, New Jersey, 2021.
2. O. A. Rakitin, in *Comprehensive Heterocyclic Chemistry IV*, eds. D. Black, J. Cossy and C. Stevens, Elsevier, Amsterdam, 2022, vol. 5, pp. 371–406.
3. N. S. Gudim, E. A. Knyazeva, L. V. Mikhalkenko, I. S. Golovanov, V. V. Popov, N. V. Obruchnikova and O. A. Rakitin, *Molecules*, 2021, **26**, 4931.
4. T. N. Chmovzh and O. A. Rakitin, *Chem. Heterocycl. Compd.*, 2022, **58**, 307.
5. E. V. Bartashevich, S. E. Mukhiddinova and V. G. Tsirelson, *Mendeleev Commun.*, 2021, **31**, 680.
6. C. P. Constantinides, M. Koyioni, F. Bazzi, M. Manoli, D. B. Lawson and P. A. Koutentis, *Molecules*, 2021, **26**, 5875.
7. E. Bartashevich, A. Stash, I. Yushina, M. Minyaev, O. Bol'shakov, O. Rakitin and V. Tsirelson, *Acta Crystallogr., Sect. B: Struct. Sci., Cryst. Eng. Mater.*, 2021, **77**, 478.
8. X. Fradera, M. A. Austen and R. F. W. Bader, *J. Phys. Chem. A*, 1999, **103**, 304.
9. A. D. Becke and K. E. Edgecombe, *J. Chem. Phys.*, 1990, **92**, 5397.
10. R. Ponec and J. Roithová, *Theor. Chem. Acc.*, 2001, **105**, 383.
11. W. L. Luken and J. C. Culberson, *Int. J. Quantum Chem.*, 1982, **22** (S16), 265.
12. G. Merino, A. Vela and T. Heine, *Chem. Rev.*, 2005, **105**, 3812.
13. F. J. Torres, L. Rincón, C. Zambrano, J. R. Mora and M. Méndez, *Int. J. Quantum Chem.*, 2019, **119**, e25763.
14. L. Rincón, F. J. Torres and R. Almeida, *Mol. Phys.*, 2018, **116**, 578.
15. R. F. W. Bader, A. Streitwieser, A. Neuhaus, K. E. Laidig and P. Speers, *J. Am. Chem. Soc.*, 1996, **118**, 4959.
16. W. L. Luken, *Croat. Chem. Acta*, 1984, **57**, 1283.
17. V. Tsirelson and A. Stash, *Acta Crystallogr., Sect. B: Struct. Sci., Cryst. Eng. Mater.*, 2021, **77**, 467.
18. E. O. Levina, M. G. Khrenova, A. A. Astakhov and V. G. Tsirelson, *J. Comput. Chem.*, 2022, **43**, 1000.
19. P. R. T. Schipper, O. V. Gritsenko and E. J. Baerends, *Phys. Rev. A: At., Mol., Opt. Phys.*, 1998, **57**, 1729.
20. E. J. Baerends and O. V. Gritsenko, *J. Phys. Chem. A*, 1997, **101**, 5383.
21. E. O. Levina, M. G. Khrenova and V. G. Tsirelson, *J. Comput. Chem.*, 2021, **42**, 870.
22. A. V. Zibarev and I. V. Beregovaya, *Rev. Heteroat. Chem.*, 1992, **7**, 171.
23. C. Outeiral, M. A. Vincent, Á. Martín Pendás and P. L. A. Popelier, *Chem. Sci.*, 2018, **9**, 5517.
24. R. G. Parr and W. Yang, *J. Am. Chem. Soc.*, 1984, **106**, 4049.
25. L. D. Betowski, M. Enlow, L. Riddick and D. H. Aue, *J. Phys. Chem. A*, 2006, **110**, 12927.

Received: 25th November 2022; Com. 22/7050